33RD INTERNATIONAL COSMIC RAY CONFERENCE, RIO DE JANEIRO 2013
THE ASTROPARTICLE PHYSICS CONFERENCE

ICRC 2013

A statistical study of Galactic SNR source spectra detected at >GeV energies

MATTHIAS MANDELARTZ[1], JULIA BECKER TJUS[1].

[1]*Theoretische Physik I, Fakultät für Physik und Astronomie, Ruhr-Universität Bochum, Germany*

matthias.mandelartz@rub.de

Abstract: Broadband modeling of 24 Galactic supernova remnants was performed using a model to test the SNRs for hadronically generated γ-rays by examining combined spectra of π^0-decay, bremsstrahlung, inverse Compton, and synchrotron radiation. For several years, measurements at super-GeV energies are performed by instruments like Fermi-LAT, H.E.S.S., MAGIC, VERITAS and Milagro and therefore, broadband SEDs exist for a growing number of SNRs. This is the first systematic statistical study of the resulting source spectra, which are reviewed individually to ascertain the origin of the gamma radiation. This allows for a combined examination to test the current models of particle acceleration in SNRs.

Keywords: Keywords

1 Introduction

Supernova remnants (SNRs) are believed to be one of the primary cosmic ray (CR) accelerators via diffusive shock acceleration [7]. These cosmic rays arriving at Earth are dominated by protons, thus their accelerators should show γ-ray signatures due to proton-proton interactions, leading to the production of pions and their decay. Although a common consensus exists whether the γ-ray emission stems from hadronic or leptonic origin, there exists a multitude of possible other scenarios which explain the emission as well as the accepted parameters (compare e.g. [3, 24]).
General information about the SNRs can be found in various catalogues [16, 13]. Supernova remnants are usually studied and modeled selecting a geometry that seems applicable to the remnant. There have been extensive studies on supernova remnants ranging from a diffusive approach [21] to the prediction of ionization signatures induced by protons if the emission is of hadronic nature [5, 29]. Here, we considered the most simplistic model to explain the spectra of supernova remnants, a power-law in the differential energy distribution of the source particles with a cut-off. This model was fitted to the broadband emission of Galactic SNRs by minimizing χ^2 at a fixed B-field to determine the origin of the gamma radiation. The assumption from [4], that the total nonthermal-energy is at a minimum — as the equipartition is generally not always be obtainanble — is used as a distinction in case multiple scenarios fit the remnant. Another disqualifier for the modeled results is the non-thermal energy threshold for the SNRs.

2 Modeling

The prevalent particle spectra at the source are assumed to exhibit a power-law behavior in the momentum of the particles [28]. The spectrum cuts off at a maximumum momentum $p_{\max}$ and a minimum momentum $p_{\min}$. The cut-off for the minimum energy is induced by a hyperbolic tangent function, as compared to the usual heaviside step function. With an arbitrary normalization constant p_0, the differential number distribution reduces to the following expression:

$$j_X(p) = a_X \left(\frac{p}{p_0}\right)^{-\alpha_X} \tanh\left(\frac{p}{p_{\min,X}}\right) \exp\left(-\frac{p}{p_{\max,X}}\right). \quad (1)$$

Here, a_X is a normalization constant of the dimensions per energy per volume and α_X the power-law index.
The maximum momentum $p_{\max}$ for protons was chosen to be 1 PeV/c to model a Galactic origin with acceleration up to the knee. In case of electron spectra the cut-off momentum was fitted to the X-ray data of the remnants. If there were no x-ray observations of the remnants, the cut-off energy was fixed to a level that the synchrotron radiation would not reach into the observable region.
The minimun momentum for protons was chosen to be 140 MeV/c in accordance with the limit derived for the ISM [26]. This is a really low lower limit, which leads to an increase in the non-thermal energy contained in protons, which might be non negligable. The non-thermal energy limit for the supernova remnant of the usual 10^{51} ergs might be too low to accomodate such a limit for the protons, so a limit for the non-thermal energy of 10^{52} ergs was used instead of the usual one to dismiss scenarios. In case of the electrons a minimum momentum of 0.85 MeV/c was used, which corresponds to the kinetic energy being about the rest mass of the particle.
The emission of photons due to interactions of the source spectra with matter can be expected. The different processes that are taken into account are the proton-proton interactions as modeled by [20], and for the electrons the emission processes as described in [8], thus synchrotron radiation, bremsstrahlung and inverse Compton radiation. The inverse Compton radiation was calculated on the cosmic microwave background only, as it should be the major contribution, as noted by [24]. Other contributions can come from e.g. scattering on the stellar radiation background. This could not be handled unifiedly for every remnant so these contributions were neglected. Bremsstrahlung was modeled assuming a standard ISM ratio, accounting for helium with an additional 1.3 factor [28].
The emission of secondary particles generated by the charged pion decay are ignored in this approach.
The resulting photon spectra, from the works of [8, 20] were fitted to the observed radiation flux of the remnants in the following way: As a first step the entire spectrum was fitted

to the radiation generated by electrons only. This ensures that a minimum magnetic field strength can be derived from this, as for higher field strengths the remnant would need less electrons to emit the observed synchrotron radiation. In the next step two seperate fits were done. After increasing the magnetic field strength, the electrons were fitted to the synchrotron observations only. Bremsstrahlung and inverse Compton radiation were then used as a background field to fit the pion decay spectra to the gamma ray observations. Bremsstrahlung as well as proton-proton interactions depend linearly on the density which were taken for each remnant from other works. Both the magnetic field strength and the density are not free parameters in the computations.
By subsequently increasing the magnetic field strength an emission profile can be generated. Different aspects can be examined this way, like the proton-to-electron ratio K_{pe} (ratio of the normalization constants of the spectra with the same momentum p_0), and the total non-thermal energy contained in the electrons, protons and the magnetic field.
This creates a batch of fits, that might all explain the SED well, although several criteria can be considered to select a likely scenario: The local proton-to-electron ratio is about 100, so it was assumed that $500 > K_{pe} > 50$. The value might also depends quite heavily on the selected density. Furthermore the theoretical SED should explain the observed one, while the total energy should be at a minimum, as with the scenario used by [4].

3 Results

As the complete profiles and resulting SEDs cannot be discussed in detail for every remnant, a constraint on two scenarios will be made.

Minimum Energy Scenario The minumum energy scenario refers to the theoretical SED configuration that explains the observed SED well, and minimizes the total non-thermal energy. This might also be a completely leptonically dominated process.

Hadronic Scenario The γ-ray SED is dominated by pion decay, and it does need less than one order of magnitude more energy than the minimum energy scenario and explains the SED as good as the minimum energy scenario.

Note that the hadronic scenario might be complementary to the minimum energy scenario — so that both scenarios are considered at the same time. The hadronic scenario is not only useful for Neutrino predictions but also usually presents to be the upper limit of the non-thermal energy contained in the remnant, while the minimum energy scenario is at its minimum.

Results for Tycho's SNR are shown in Figures 1, 2, and 3. Tycho had a unique jump in its spectrum due to the algorithm first starting out with a steep power-law index of about 3 and when the TeV gamma ray emission could not be sufficiently be explained by it anymore the algorithm jumped and adopted an index of about 2.3. The results obtained by modeling Tycho's SNR generally match with other hadronic models of this SNR [24].
A large amount of modeled supernova remnants have their derived spectral indices attached with an error of $0.1 - 0.2$. The bin size for the power-law index histogram was adjusted to 0.2 accordingly. The electron power-law index shows the expected distribution and peaks sharply around

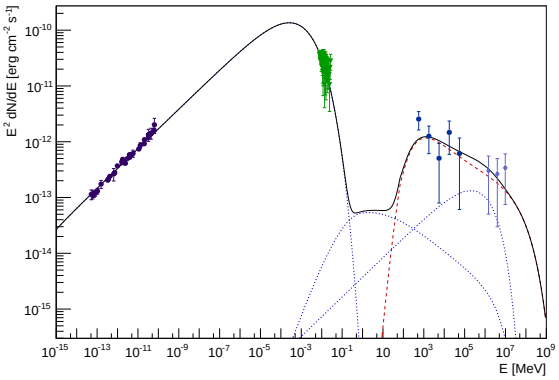

Figure 1: Tycho's SNR at the minimum energy scenario of about $B = 100\,\mu$G. Leptonic radiation is displayed as dotted lines, hadronic emission as dashed lines. Measurements are from [1, 15, 24, 27].

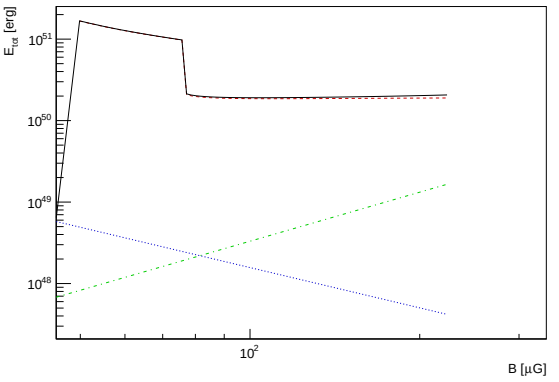

Figure 2: Non-thermal energy budget of Tycho depending on the magnetic field. Protons are dashed, electrons are dotted and the magnetic field energy is dashed-dotted. The jump in the non-thermal energy occurs due to a jump in the proton power-law index while modeling (from ~ 3 to ~ 2.3).

a value of 2, which is expected for strong shock [6], see Figure 4.
The histogram of the fitted proton power-law indices, displayed in Figure 5, does not peak sharply around 2. Both the hadronic as well as the minimum energy scenario are visible. So that the doubly peaked structure that is visible is an effect that is not due to selection effects, and the actual distribution can be expected to lie in between the hadronic and the minimum energy scenario.
The distribution has its first peak for power-law indices $2.1 < \alpha_p < 2.3$, furthermore there is a second unexpected peak for power-law indices $\alpha_p \gtrsim 2.6$. This hints that these supernova remnants are different from the other SNRs, which are contained in the first peak. Thus two kinds of hadronically dominated SNRs can be identified, based on their γ-ray SED:

Class I A power-law index of $2.0 < \alpha_p < 2.3$. This class is from its current SED in the MeV–TeV domain indistinguishable from the shape of a bremsstrahlung dominated spectrum.

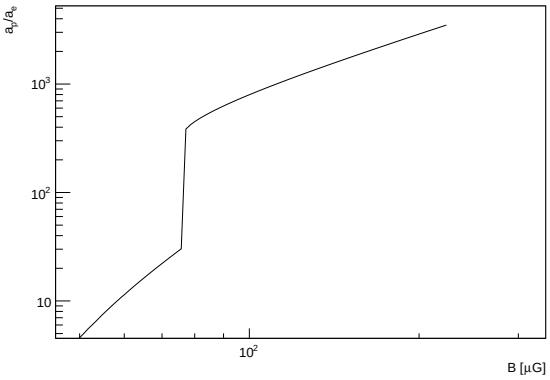

Figure 3: The proton-to-electron ratio K_{pe} over the magnetic field for Tycho. The jump in the spectral index is here visible, too.

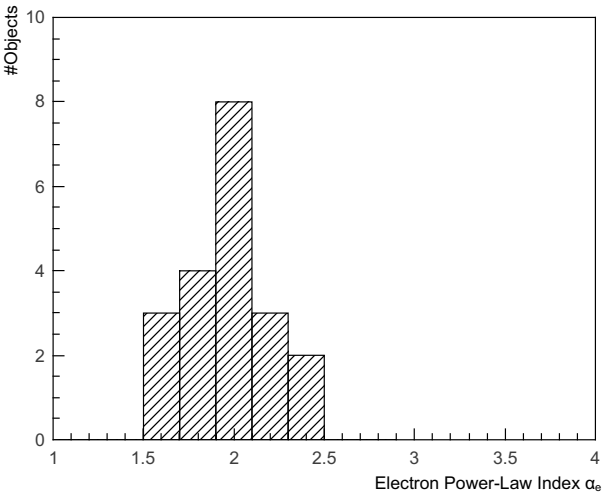

Figure 4: Electron power-law indices of the fitted synchrotron SEDs.

Class II A power-law index of $\alpha_p \gtrsim 2.6$. A sharp hadronic peak with a sudden decline exists in the MeV–GeV domain. The GeV–TeV domain is commonly dominated by bremsstrahlung or inverse Compton radiation in those cases.

The existance of those two classes still has to be confirmed by more statistics. These classes have different properties concerning the resulting theoretical SEDs. Class I usually has a letonically generated MeV–GeV gamma ray SED, and the hadronic nature of the MeV–TeV spectrum can only be confirmed by TeV measurements. These measurements have to be taken at energies higher than the cut-off energy of the electron source spectrum which highest possible values are around 50–100 TeV.
From the modeling of Class II SNRs it is not clear wheather the proton power-law index is really that steep or if the spectrum follows a different shape. The deviation cannot be attributed to aging effects, but might be due to other effects like diffusion.
In Figure 6 the proton spectral index is plotted against the electron spectral index. The respective errors from the modeling are visible in the graphic. Usually empirical data in nature rarely follow power-laws with an index smaller

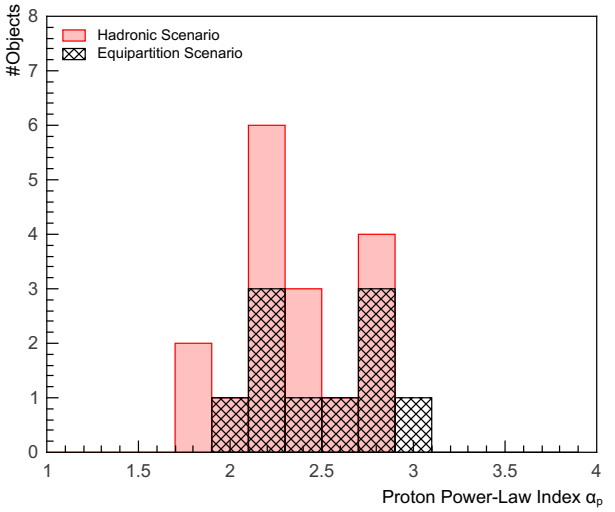

Figure 5: Proton Power-Law indices of the fitted γ-ray SEDs, in the hadronic and the equipartition/minimum energy scenario.

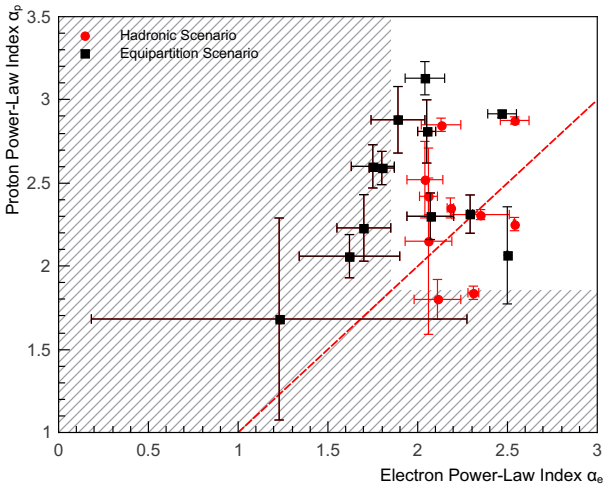

Figure 6: Proton power-law index vs electron power-law index in the minimum energy/equipartition scenario and the hadronic case.

than 2 [9], so that the region with an index smaller than 1.85 was considered as unphysical parameter space, crossed out in gray in the graph; but all modeled supernova remnants are compatible with physics considering their 1σ error bars. Generally it is observable from the graphic that the proton power-law index tends to be steeper than the electron power-law index. This raises the question of the nature of the steeper proton power-law compared to the electron power-law, as shown in Figure 6. There are various explanations ranging from diffusion [2, 30] to deteriorated particle confinement [22]. There are various suggested mechanisms that lead to spectral steepenings, but which of them are realized or responsible for the observed spectrum is not clear at this point.
The modeling would be far more accurate, if the data of SNRs would be increased by more observations. Especially the energy range of 0.1 – 100 MeV which would be crucial to differentiate if the Fermi-LAT data is indeed bremsstrahlung, and the energy range beyond H.E.S.S.

would help greatly too, as H.E.S.S. currently observes in the energy range where the electron cut-off could occur in at least some cases. Further observations in the energy range higher than H.E.S.S. by telescopes like CTA and HAWC [11] would help to seperate the hadronic part from the leptonic radiation further.
Another option to seperate the hadronic part from the leptonic part is by using neutrino observations as the basis to model the hadronic emission from the remnant. With the current state of the model the hadronic neutrino emission can be estimated and can be tested against observations from the telescopes to either get a detection or to derive upper-limits for the current state of the flux.
Oscilated fluxes from the modeled supernova remnants can be seen in Figure 7. Declination-averaged point source sensitivities of neutrino observatories (IceCube [18]) have been added to the plot. For the southern sky plot see [23].

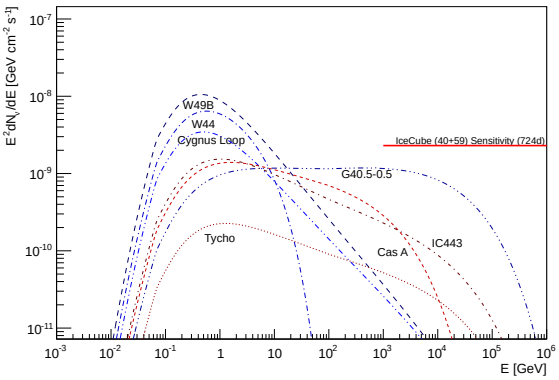

Figure 7: Possible neutrino emission of Galactic SNRs in the hadronic scenario.

4 Summary

Galactic SNRs were modeled in this work to test them wheather their emission is definite of hadronic nature, and it was found that usually simple power-laws with cut-offs for electrons and protons suffice to explain the observed radiation. The distribution of the hadronic power-law indices allowed to group the remnants into two categories:

Class I A power-law index of $2.0 < \alpha_p < 2.3$. This class is from its current SED in the MeV–TeV domain indistinguishable from the shape of a bremsstrahlung dominated spectrum.

Class II A power-law index of $\alpha_p \gtrsim 2.6$. A sharp hadronic peak with a sudden decline exists in the MeV–GeV domain. The GeV–TeV domain is commonly dominated by bremsstrahlung or inverse Compton radiation in those cases.

Class II seems to be common among SNRs that are interacting or might interact with molecular clouds a morphological origin was not examined in this work. A SNR interacting with a molecular cloud is not a guarantee for the remnant to appear in Class II.
The letptonic emission in the MeV–TeV range is often dominated by bremsstrahlung, a high density easily suppresses the pion decay emission, too, however there are not many bremsstrahlung emission dominant models in literature. For the bremsstrahlung to be dominant a power-law index lower than the proton spectrum is needed, in addition to a high density ($> 50\,\mathrm{cm}^{-3}$). This condition however is easily fulfilled, as the electron spectrum scatters around the value of 2.

Acknowledgment: JBT and MM acknowledge the support from the DFG in the framework of the research group FOR1048 on "Instabilities, turbulence and transport in cosmic magnetic fields" and from the Research Department of Plasmas with Complex Interactions (Bochum) and from the MERCUR Project Pr-2012-0008.

References

[1] Acciari, V.A. et al. 2011, Astrophysical Journal, Letters, 730, L20.
[2] Aharonian, F.A. and Atoyan, A.M. 1996, Astronomy and Astrophysics, 309, 917.
[3] Atoyan, A., & Dermer, C. D. 2012, Astrophysical Journal, Letters, 749, L26.
[4] Beck, R. and Krause, M. 2005, Astronomische Nachrichten, 326, 414.
[5] Becker, J.K. et al. 2011, Astrophysical Journal, Letters, 739, L43.
[6] Bell, A.R. 1978, Monthly Notices of the RAS, 182, 147.
[7] Blandford, R.D. and Ostriker, J.P. 1978, Astrophysical Journal, Letters, 221, L29.
[8] Blumenthal, G.R. and Gould, R.J. 1970, Rev. Mod. Phys., 42, 237.
[9] Clauset, A. et al. 2009, SIAM Review, 51, 661.
[10] Cox, D.P. 1972, Astrophysical Journal, 178, 159.
[11] Dubus, G. et al. 2012, arXiv:1208.5686.
[12] Erickson, W.C. and Mahoney, M.J. 1985, Astrophysical Journal, 290, 596.
[13] Ferrand, G., & Safi-Harb, S. 2012, Advances in Space Research, 49, 1313.
[14] Galassi, M. et al. 2009, GNU Scientific Library Reference Manual (Network Theory).
[15] Giordano, F. et al. 2012, Astrophysical Journal, Letters, 744, L2.
[16] Green, D.A. 2009, Bulletin of the Astronomical Society of India, 37, 45.
[17] Hillas, A.M. 2005, J. of Phys. G: Nucl. Phys., 31, 95.
[18] Kappes, A. 2012, arXiv:1209.5855
[19] Katz, U.F. and Spiering, C. 2012, Progress in Particle and Nuclear Physics, 67, 651.
[20] Kelner, S.R., Aharonian, F.A., & Bugayov, V.V. 2006, Physical Review D, 74, 034018
[21] Li, H. and Chen, Y. 2012, Monthly Notices of the RAS, 421, 935.
[22] Malkov, M.A., Diamond, P.H., and Sagdeev, R.Z. 2012, Physics of Plasmas, 19, 082901.
[23] Mandelartz, M., & Becker Tjus, J. 2013, arXiv:1301.2437
[24] Morlino, G. and Caprioli, D. 2012, Astronomy and Astrophysics, 538, A81.
[25] Nelder, G.R. and Mead, R.J. 1965, The Computer Journal, 7, 308.
[26] Padovani, M. et al. 2009, Astronomy and Astrophysics, 501, 619.
[27] Reynolds, S.P. and Ellison, D.C. 1992, Astrophysical Journal, Letters, 399, L75.
[28] Schlickeiser, R. 2002, Cosmic Ray Astrophysics (Springer).
[29] Schuppan, F. et al. 2012, Astronomy and Astrophysics, 541, A126.
[30] Strong, A.W., Moskalenko, I.V., and Ptuskin, V.S. 2007, Annual Review of Nuclear and Particle Science, 57, 285.
[31] Williams, B.J. et al. 2011, Astrophysical Journal, 741, 96.
[32] Yang, J. et al. 2006, Chinese Journal of Astronomy and Astrophysics, 6, 210.
[33] Zirakashvili, V.N. and Aharonian, F. 2007, Astronomy and Astrophysics, 465, 695.